Molecular Catalysis 505 (2021) 111514

Contents lists available at ScienceDirect

Molecular Catalysis

journal homepage: www.journals.elsevier.com/molecular-catalysis

Highly active CuZn/SBA-15 catalyst for methanol dehydrogenation to methyl formate: Influence of ZnO promoter

Na Wang [a,b], Yanhong Quan [a,b], Jinxian Zhao [a,b], Haixia Li [a,b], Jun Ren [a,b,*]

[a] State Key Laboratory of Clean and Efficient Coal Utilization, Taiyuan University of Technology,Taiyuan 030024, China
[b] Key Laboratory of Coal Science and Technology (Taiyuan University of Technology), Ministry of Education

ARTICLE INFO

Keywords:
SBA-15
Methyl formate
ZnO
Cu species
Dehydrogenation

ABSTRACT

Stable and efficient Cu/SBA-15 and *x*CuZn/SBA-15 ($x = 5$, 10 and 15) in methanol dehydrogenation to methyl formate (MF) are prepared through a double-solvent impregnation (DI) method. Among all catalysts, 10CuZn/SBA-15 shows the highest catalytic performance with selectivity to MF about 88.1 % and methanol conversion of 31.1 %, which is attributed to the well-dispersed Cu particles and high ratio of $Cu^{\circ}/(Cu^{\circ} + Cu^{+})$. The proper amount of ZnO could improve dispersion of Cu because of its geometrical spacer, inhibiting growth of Cu particle, and the best dispersion is achieved in 10CuZn/SBA-15. Furthermore, the $Cu^{\circ}/(Cu^{\circ} + Cu^{+})$ ratio is greatly promoted with the assistance of ZnO, attributed to Cu-ZnO interaction, which reaches maxima of 53.3 % at a Cu/Zn mole ratio of 10. Specially, the optimized catalyst shows evident suitability at high temperature for methanol dehydrogenation reactions along with high level of conversion and selectivity for 100 h. Overall, our findings reveal that modification by the appropriate amount of ZnO in Cu-based catalyst has a positive impact on obtaining MF for the methanol dehydrogenation.

1. Introduction

Methyl formate (MF) is an important and indispensable component of numerous chemical products in C1 chemistry, such as formic acid, acetic acid, propionic acid, formamide, dimethyl formamide, and ethylene glycol [1–3]. MF can be successfully synthesized by several processes, including methanol carbonylation [4], oxidative coupling of methanol [5], methanol dehydrogenation [6,7], direct synthesis from CO and H_2 [8] as well as hydrogenation of CO_2 [9]. Among these processes, the methanol dehydrogenation has been deemed to have great commercial prospects on account of important merits including simple procedures, abundant raw materials and recyclable by-product H_2 [10].

Methanol conversion could be promoted at the high temperature since methanol dehydrogenation reaction to produce MF is endothermic. However, the rising temperature will lead to the further decomposition of MF to CO, resulting in the decrease of its selectivity. Thus, the improvement of methanol conversion and MF selectivity are not achieved at the same time, accounting for the selection and design of catalyst is crucial. It has been demonstrated that both noble metal and transition metal as active catalysts are used for this reaction. The noble metal catalysts exhibit excellent catalytic performance [11], but they are unsuitable widespread in industry because of their high price and deactivation. By comparison, Cu-based catalysts are the appropriate candidates for methanol dehydrogenation due to its economical and prominent performance [12–15], in which Cu° as the main active species has been got consensus on the basis of a large number of reports [16–18]. For Cu-based catalysts, the Cu° facilitate dissociates the oxygen-hydrogen of methanol to methoxyl group and further to formaldehyde group through dissociate carbon-hydrogen bonds, but the Cu^{+} sites lead to formaldehyde group decompose rapidly generate to CO and H_2 [19]. In other words, the Cu° is beneficial for the formation of MF, while Cu^{+} is helpful to formation of CO. Thus, the control on concentration of Cu° is one of the effective strategies promoting the catalytic performance for methanol dehydrogenation. The previous studies showed that adding additives such as ZnO [20–22], Be [23–25] and Ce [26] could effectively change the ratio of Cu° and thus influence the catalytic performance and stability in the reaction because of the strong interaction between surface metals. Especially, the performance of ZnO modified Cu-based catalysts improves significantly, thus the role of ZnO additives has become research hotspot. Huang et al. [27] proposed that additives of ZnO can improve the MF selectivity from 49.5 % to 79.8 %.

Besides the concentration of Cu°, the dispersion of Cu nanoparticles

* Corresponding author.
E-mail addresses: renjun@tyut.edu.cn, 2018879598@qq.com (J. Ren).

https://doi.org/10.1016/j.mcat.2021.111514
Received 16 November 2020; Received in revised form 2 March 2021; Accepted 4 March 2021
Available online 21 March 2021

is an important factor to consider for the dehydrogenation reaction due to sintering easily for CuO or Cu nanoparticles during the thermal treatments. It has been proved that SBA-15 is a good candidate as support for well dispersing Cu nanoparticles [28,29], which can be ascribed to space limitation of its regular channels inhibiting active species from agglomeration [30] and high specific surface area enhancing the dispersion of Cu particles [31].

Recently, the ZnO modified Cu-based catalysts exhibit excellent catalytic in various catalytic reactions, such as dimethyl ether steam reforming [26], dimethyl ether synthesis, methanol synthesis [32], and so on [33]. The role of ZnO has been focused and has increasing attention by numerous researchers. Up to now, two main hypotheses are greatly accepted: one is that ZnO as a spacial barrier helps to increase the Cu particles dispersion, the another one is that it acts as the active species in the terms of Cu-Zn alloy [34]. Huang et al. [27] found that adding ZnO is beneficial to enhance the Cu nanoparticles dispersion and produce Cu-ZnO interaction, thus improving activity of catalyst in methanol dehydrogenation. Besides, Cu-based catalyst modified by ZnO possesses the superior stability to ZnO-free ones, attributing to good dispersity of Cu nanoparticles keep in the reaction process provided by inhibition of ZnO from Cu agglomeration. Nevertheless, systematic research about the effect of ZnO modified Cu-based catalyst for methanol dehydrogenation is seldom reported.

With the aim of optimizing the catalytic performance, ZnO is used as an additive to modify the Cu-based catalysts to obtain more effective and stable catalysts. In this article, highly dispersed *x*CuZn/SBA-15 catalyst synthesized through DI method was used to catalyze methanol dehydrogenation. The physical and chemical properties of samples were investigated with the help of several characterization techniques and their catalytic performance was studied. The structure-function relationship was explored. The role of ZnO was made detailed discussion.

2. Experimental

2.1. Catalyst preparation

The *x*CuZn/SBA-15 and Cu/SBA-15 catalysts with Cu loading of 20 wt% were synthesized by the double-solvent impregnation method. 1 g of SBA-15 was ultrasonically dispersed in 30 mL of hexane. After adding 10 mL of aqueous solution containing certain amount of $Cu(NO_3)_2{\cdot}3H_2O$ and $Zn(NO_3)_2{\cdot}6H_2O$ into the suspension, the resultant solution was stirred at 35 °C for 2 h and then filtrated and dried at 80 °C for 12 h in air. At last, the obtained solid was reduced by H_2/N_2 flow at 300 °C for 2 h in a tube furnace. The reduced catalysts were denoted as *x*CuZn/SBA-15 (x = 5, 10 and 15), in which x means the mole ratio of Cu/Zn. The Cu/SBA-15 catalyst (20 wt% Cu loading) was prepared by the same procedure without the use of $Zn(NO_3)_2{\cdot}6H_2O$.

2.2. Catalysts characterization

Transmission electron microscopy (TEM) was obtained through a JEOL-2100 F electron microscope with X-ray energy-dispersive-spectrometer (EDS). X-ray diffraction (XRD) was conducted on a Rigaku D/max 2500 diffraction using Cu Kα radiation with the 2θ range from 5 to 85°. The nitrogen physisorption was determined on a Beishide 3H-2000PS2 instrument. The specific surface area (S_{BET}), pore diameter (D_P) and pore volume (V_P) were obtained through Brunauer-Emmett-Teller (BET) and Barrett-Joyner-Halenda model. X-ray photoelectron spectra (XPS) was collected through Thermo ESCALAB 250 spectrometer with an Al Kα X-ray source. H_2 temperature-programmed reduction (H_2-TPR), H_2-N_2O titration and CH_3OH temperature-programmed desorption (CH_3OH-TPD) was tested on a XianQuan TP-5080 equipment. H_2-TPR were monitored by thermal conductivity detector with pretreatment under Ar flow at 200 °C for 60 min before reducing by 30 % H_2/Ar from 30 °C to 500 °C (10 °C min^{-1}). For H_2-N_2O titration, catalysts were reduced at 450 °C under 30 % H_2/Ar and then cooled to 30 °C with Ar, followed by exposure to 30 % N_2O/Ar keeping 30 min. The next procedure is the same as that of the H_2-TPR experiment. The operation of CH_3OH-TPD was as follows. The samples were degassed at 300 °C in He flow for 60 min and afterwards kept at 100 °C, before methanol introduced He was used as a carrier gas. After He was used to wash away the physical molecules on the surface, the temperature was increased until 900 °C (10 °C min^{-1}).

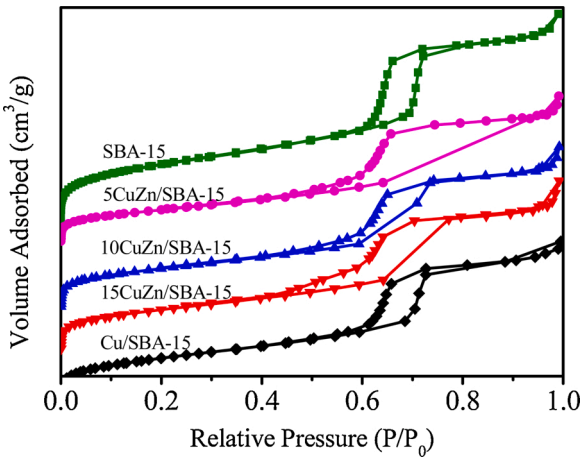

Fig. 1. N_2 physisorption isotherms of reduced catalysts.

2.3. Catalyst evaluations

In this study, methanol dehydrogenation to MF was conducted in a fixed-bed reactor (500 mm × 8 mm) filled with 0.3 g catalyst sample diluted with 3 g of quartz sand at pressure of 0.2 Mpa with reaction temperature of 300 °C. Methanol was injected (0.05 mL min^{-1}), which is vaporized in the preheater and then fed into reactor for catalytic dehydrogenation, using N_2 as a carrier gas (30 mL min^{-1}). After condensation in condenser, the products were collected and then monitored through gas chromatograph (GC-920, Shanghai Haixin) using thermal conductivity and flame ionization detectors. The MeOH conversion (C_{MeOH}, %), MF selectivity (S_{MF}, %), CO_2 selectivity (S_{CO2}, %), CO selectivity (S_{CO}, %) and MF yield (Y_{MF}, %) were calculated according to the following equations:

$$C_{MeOH} = \frac{2 \times n_{MF} + n_{CO2} + n_{CO}}{n_{MeOH} + 2 \times n_{MF} + n_{CO2} + n_{CO}} \times 100\%$$

$$S_{MF} = \frac{2 \times n_{MF}}{2 \times n_{MF} + n_{CO2} + n_{CO}} \times 100\%$$

Table 1
Textural properties of Cu/SBA-15 and *x*CuZn/SBA-15 catalysts.

Catalysts	S_{BET}[a] (m^2/g)	V_P[a] (cm^3/g)	D_P[a] (nm)	D_{Cu}[b] (%)	S^0_{Cu}[b] (m^2/g)	X^0_{Cu}[c] (%)
SBA-15	624	0.91	6.0	–	–	–
Cu/SBA-15	464	0.78	5.8	35.8	242.2	45.3
15CuZn/SBA-15	431	0.75	5.7	36.3	245.5	51.0
10CuZn/SBA-15	419	0.72	5.8	40.1	271.5	53.3
5CuZn/SBA-15	347	0.65	5.7	34.7	234.7	52.1
SiO_2	347	1.14	13.2	–	–	–
10CuZn/SiO_2	277	1.76	25.5	21.7	–	–

[a] The S_{BET}, V_P and D_P determined by N_2 adsorption-desorption.
[b] The D_{Cu} and S^0_{Cu} on the surface calculated by N_2O chemisorption.
[c] The X^0_{Cu} calculate by Cu LMM AXES spectra.

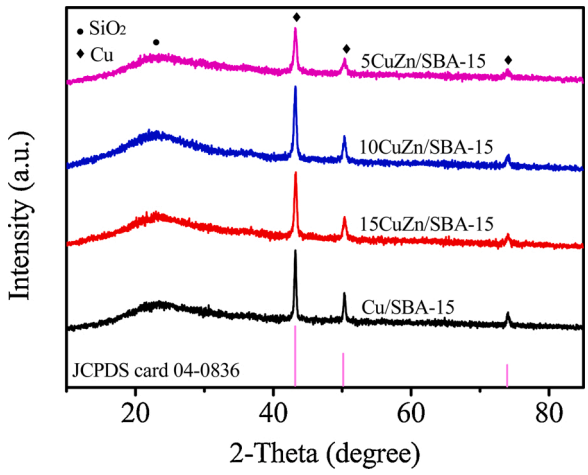

Fig. 2. XRD patterns of reduced catalysts.

$$S_{CO2} = \frac{n_{CO2}}{2 \times n_{MF} + n_{CO2} + n_{CO}} \times 100\%$$

$$S_{CO} = \frac{n_{CO}}{2 \times n_{MF} + n_{CO2} + n_{CO}} \times 100\%$$

$$Y_{MF} = C_{MeOH} \times S_{MF} \times 100\%$$

3. Results and discussions

3.1. Physicochemical properties of catalysts

3.1.1. Textural properties

The N_2 physisorption of all reduced catalysts are illustrated in Fig. 1 and the textural properties of samples are list in Table 1. All samples exhibit the IV isotherm with H1 hysteresis loops, which indicates mesoporous structure of SBA-15 is maintained in all samples after the introduction of Cu and ZnO species. Obviously in Table 1, S_{BET} and V_P of *x*CuZn/SBA-15 catalyst slowly decrease as increment of ZnO content, implying that ZnO particles covering and clogging the pore channels of SBA-15 supports during the process of catalyst preparation [21].

3.1.2. Crystalline phase and morphology

The XRD in Fig. 2 evidence the structures of reduced catalysts. The wide peak is detected at 22.5° in all samples, which can be assigned to the feature peak of amorphous SiO_2. The sharp diffraction characteristic at 43.1°, 50.2° and 74.1° are attributed to metallic Cu (111, 200, 220) [28], which may be due to the Cu^{2+} is reduced. In addition to this, no obvious characteristic for zinc oxide are discovered among all catalysts even if Cu/Zn is as low as 5, probably due to the high dispersion and uniform distribution of the ZnO species generated by a double-solvent impregnation method. Laugel et al. [35] proved that the DI method is helpful to enhance the dispersion of these metal oxide nanoparticles.

Fig. 3 demonstrates the TEM pictures for four reduced samples (left) and corresponding size distribution histograms of Cu nanoparticles (right). All samples display well-dispersed of Cu particles on the SBA-15 supports. The notable physical difference among the four catalysts lie in the mean size of Cu nanoparticles, which firstly decrease and then increase with the increase of ZnO content, and reach a minimum value of 7.5 nm at a Cu/Zn molar ratio of 10. According to the HRTEM image (insets in Fig. 3c), zinc oxide obviously acts as a physical spacer to separate copper particles [36–39]. Therefore, it can be concluded that the addition of an appropriate amount of ZnO could effectively inhibit Cu nanoparticles from agglomeration during the preparation process of *x*CuZn/SBA-15. Fig. 4 displays the corresponding element images of reduced 10CuZn/SBA-15 catalysts. It is observed that the signal distribution of Cu and ZnO species are relatively uniform and well-dispersed, suggesting that metal compositions are effectively dispersed on the surface of SBA-15, consistent with the findings of TEM and XRD characterization.

For Cu-based catalysts, the Cu dispersion (D_{Cu}) is one of significant factors affecting catalytic performance of the methanol dehydrogenation to MF [27]. The Cu dispersion of the Cu/SBA-15 and *x*CuZn/SBA-15 catalysts is summarized in Table 1. It can be seen that the D_{Cu} value firstly increase and then decrease with the increment of ZnO content, and achieved the maximum of 40.1 % in the 10CuZn/SBA-15 catalyst, which is in agreement with the TEM results. As for 15CuZn/SBA-15, the ZnO content is too low to isolate copper particles abundantly. While, the ZnO content is relatively high in the 5CuZn/SBA-15 catalyst, and the copper would squeeze together and thus led to a decrease of Cu dispersion. Combined with the TEM and N_2O titration results, it is believed that an appropriate amount of ZnO acts as a physical barrier, isolating copper species so as to improve the Cu dispersion in the *x*CuZn/SBA-15 catalysts [38].

Fig. 5 shows the H_2-TPR profiles for different catalysts. The 15CuZn/SBA-15 and 5CuZn/SBA-15 catalysts present two obvious reduction processes specified as low-temperature peak and high-temperature peak, which can be assigned to reduction of well-dispersed CuO nanoparticles to Cu° as well as bulk CuO to Cu^+ and Cu°, respectively [22, 40–42]. Nevertheless, the reduction peak of large CuO particles in 10CuZn/SBA-15 is hard to be distinguished, which might be attributed to a more uniform distribution of copper nanoparticles as confirmed by the TEM analysis. Thus, it can be known that the 10CuZn/SBA-15 catalyst possess a higher reducibility compared with the other catalysts. With the increment of ZnO loading, the reduction peak shifts towards a higher temperature, which may be due to the presence of a specific type of Cu-ZnO interaction [21,43].

3.1.3. Surface chemical states

Fig. 6a shows the Cu 2p XPS results of reduced samples. Typically, the binding energy (BE) Cu $2p_{3/2}$ peak at around 934.2 eV and the satellite peak at 943.2 eV confirm the presence of Cu^{2+} species [44,45]. In Fig. 6a, only the Cu $2p_{1/2}$ BE at 952.4 eV and Cu $2p_{3/2}$ BE at 932.6 eV belonging to Cu^+ and/or Cu° are found [46], which indicates that high valence state copper are reduced to low valence state [47]. From the Fig. 6b, the asymmetrical and broad peak is detected and divided to the two symmetric peaks center at 916.1 and 912.2 eV, assigning to Cu° and Cu^+, conventionally. The relative proportion of Cu° and Cu^+ is computed based on Cu LMM XAES spectra [48,49], and relevant data is shown in Table 1. The Cu° percentage (X_{Cu}°) first increases and then decreases with increasing of ZnO loading, indicating it is greatly affected by the ZnO content of this catalyst. And the 10CuZn/SBA-15 catalyst owns the highest ratio of Cu°/(Cu° + Cu^+) of 53.3 %.

The Zn 2p XPS spectra of the *x*CuZn/SBA-15 catalysts are shown in Fig. 7. The peak observed at 1022.4 eV could be assigned to Zn $2p_{3/2}$ electrons, which is greater than the value of Zn^{2+} (1021.2 eV) in the reference ZnO as reported [22]. This finding indicates that the ZnO in the *x*CuZn/SBA-15 catalysts should be electron-deficient compared with pure ZnO species [50,51]. It is inferred reasonably that ZnO serves as an electron donor promotes the transfer of electron in the reduction process, which is beneficial to the reduction of copper and thus increase the Cu° concentration as confirmed by Cu LMM XAES spectra (Table 1). In summary, it is known that ZnO functions as both structural promoter and electronic promoter in the *x*CuZn/SBA-15 catalysts. Furthermore, the catalytic performance could be promoted through controlling of ZnO loading, since Cu° as an active species and it is of great significance in methanol dehydrogenation.

Cu° specific surface area (S_{Cu}°) determines by H_2-N_2O titration. From Table 1, the S_{Cu}° first increases, reaching the maximum value of 271.5 m^2/g when the mola ratio of Cu to Zn is 10, and then decline as the ZnO content raise. The observation indicates that the appropriate amount of ZnO could effectually enhance the Cu dispersion and thus increase S_{Cu}°, while large Cu nanoparticles could be formed and thus result in

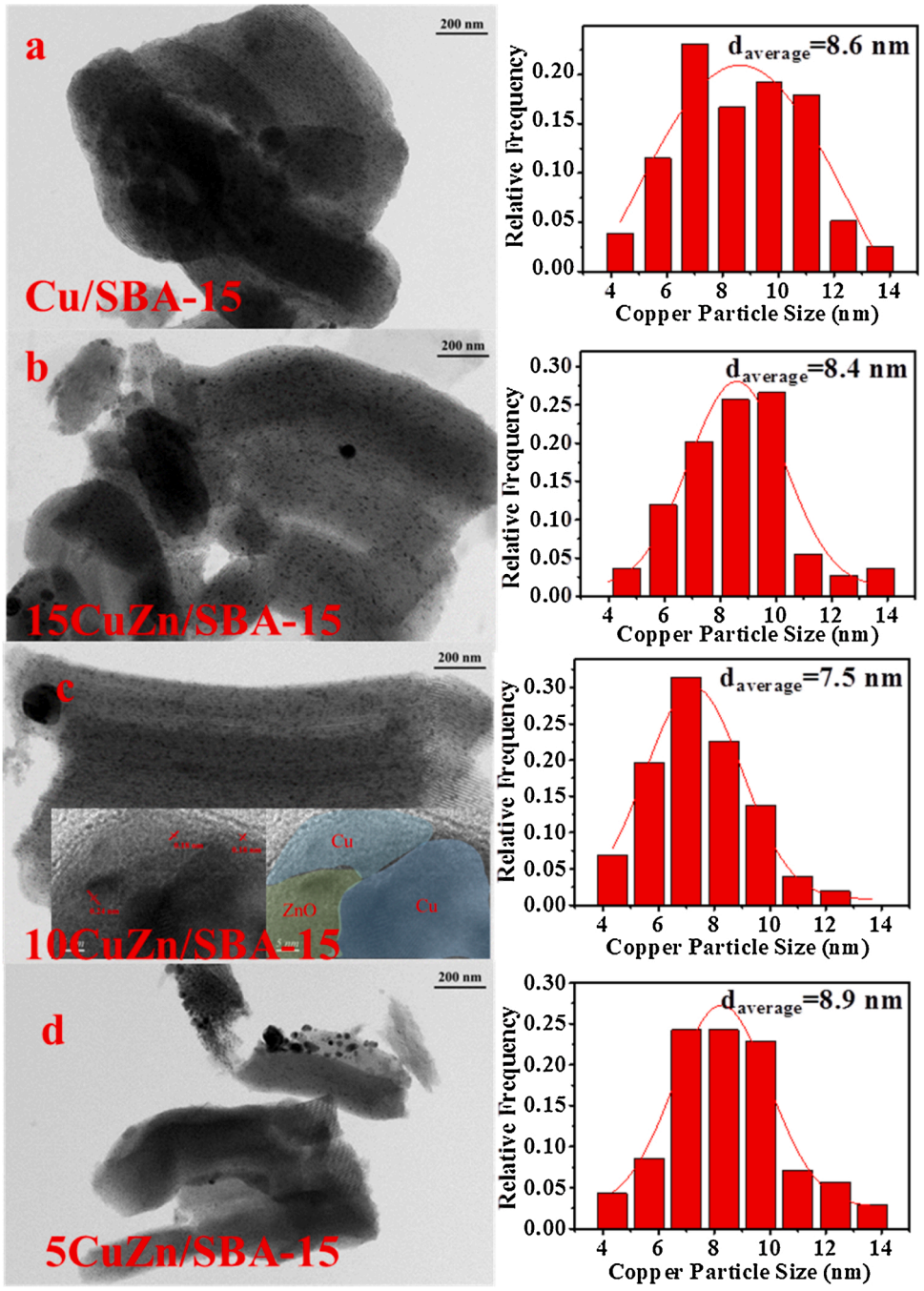

Fig. 3. TEM patterns of reduced catalysts and the corresponding size distribution histograms of Cu particles.

decreasing of Cu° surface area as excess ZnO is added [22].

3.1.4. CH_3OH-TPD

Fig. 8 displays the CH_3OH-TPD curves for these reduced catalysts. There are three desorption peaks at 50−280 °C, 280−370 °C and 370−500 °C, respectively. Nevertheless, only the medium-strong desorption segment (280−370 °C) is major concern due to the reaction temperature of 300 °C in this work. In this range, the desorption peak area is greatly affected from the ZnO introduction and it first increases and then decreases with increasing ZnO, implying the ZnO loading in the Cu-based catalysts have an important impact on the CH_3OH adsorption capacity. It is also found that the trend of CH_3OH adsorption capacity is consistent with that of the S_{Cu°, suggesting Cu° species provide the adsorption sites and play the significant role in adsorption of CH_3OH in the reaction process [19]. Obviously, the largest desorption peak area appears in 10CuZn/SBA-15, ascribed to its largest surface area of Cu° species (271.5 m^2/g), which is indicative of the strongest adsorption capacity of CH_3OH. In a word, CH_3OH adsorption capacity of *x*CuZn/SBA-15 is capable to be enhanced greatly by surface area of Cu° species results from the appropriate amount of ZnO, conducive to promoting the catalytic performance in methanol dehydrogenation reaction.

3.2. Activity of catalysts

Table 2 shows the catalytic performance of reduced Cu/SBA-15 and *x*CuZn/SBA-15 catalysts for methanol dehydrogenation in 300 °C. Cu/SBA-15 shows a relatively low methanol conversion (C_{MeOH}) of 17.8 %

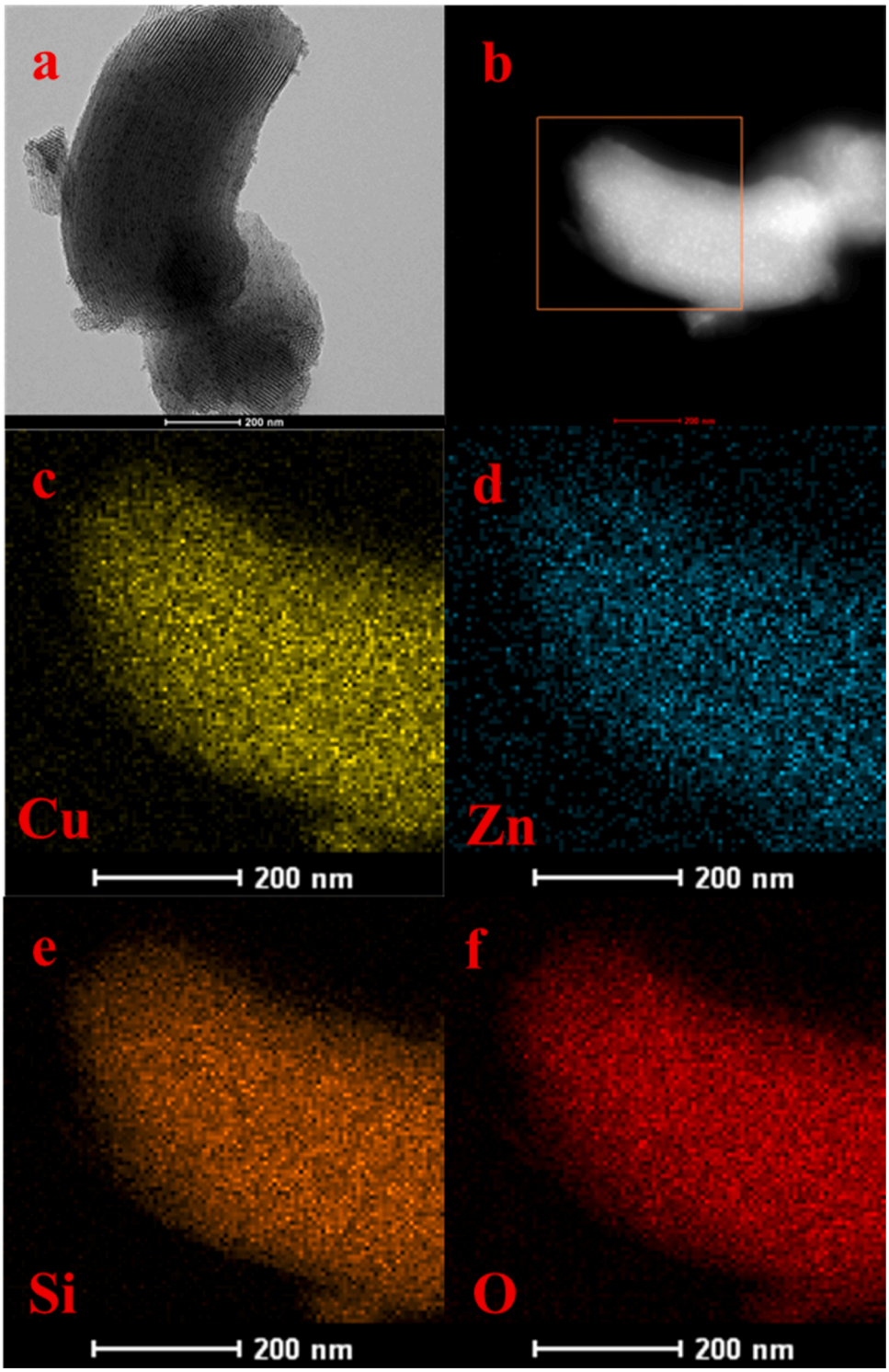

Fig. 4. Elemental mappings of reduced 10CuZn/SBA-15: (a) STEM, (b) selection precinct, (c-f) EDS elemental mapping.

and MF selectivity (S_{MF}) of 46.5 %. Compared with Cu/SBA-15, the activity of *x*CuZn/SBA-15 is enhanced markedly at different degree depending on the ZnO amount. Among all these catalysts, the 10CuZn/SBA-15 shows the best catalytic performance with C_{MeOH} of 31.1 % and S_{MF} of 88.1 % superior to the results reported.

With increasing ZnO content, C_{MeOH} increases until it reaches a maximum for 10CuZn/SBA-15, and then decreases. The S_{MF} presents a similar trend with C_{MeOH}, whereas the opposite trend for S_{CO} is observed, which implies that side reaction producing by-products of CO is inhibited effectively through the introduction of ZnO. The possible reaction path of methanol dehydrogenation to MF is as follows. Firstly, the O—H bond in CH_3OH is cleavage to CH_3O species. Then, the C—H bond of CH_3O is dissociated to produce HCHO intermediate, which is the rate-limiting step of MF formation. Finally, MF is produced through the CH_3O species reacting with HCHO (hemiacetal route) [52] or HCHO dimerization (Tishchenko mechanism) [53]. During the process of methanol dehydrogenation, the Cu° promote the cleavage of the O—H bond in CH_3OH to CH_3O and further to form HCHO by promoting the

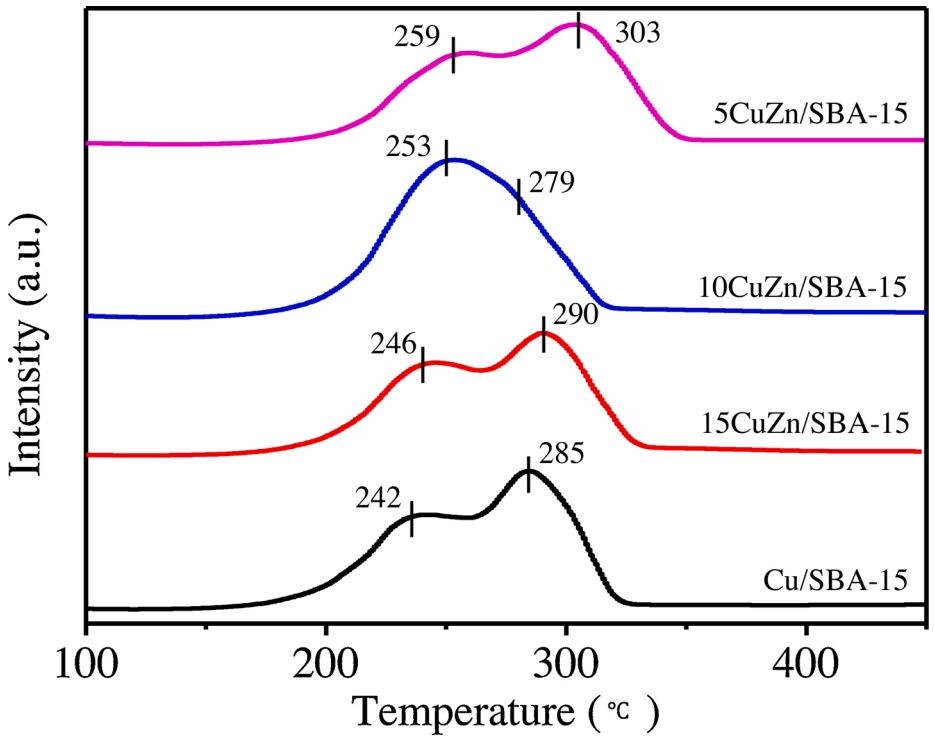

Fig. 5. H_2-TPR curves of unreduced catalysts.

dissociate of C—H bond, whereas Cu^+ sites cause rapid decomposition of HCHO to CO and H_2 [19]. It is confirmed that Cu° species contributed to the formation of MF, while Cu^+ species help to produce CO. It can deduce that both the improvement of S_{MF} and the declining of S_{CO} resulted from the increase of Cu° percentage through the ZnO introduction.

It should be mentioned that the variation of C_{MeOH} and S_{MF} for *x*CuZn/SBA-15 is consistent with the trend of Cu dispersion, the Cu° surface area as well as $Cu^\circ/(Cu^\circ + Cu^+)$ ratio see from Table 1, and opposite to the trend of Cu particles size proved by the TEM and H_2-TPR consequences, which suggests that the improvement of activity should be corresponding closely to the physicochemical property of Cu species derived from the introduction of moderate ZnO. According to previous literatures, the copper dispersion and $Cu^\circ/(Cu^\circ + Cu^+)$ ratio could be considered as the crucial factor affecting the activity. Proved by N_2O titraotion result and TEM result, the Cu dispersion of 10CuZn/SBA-15 is largest, which can provide more active sites (proved by Cu° specific surface area) and contribute to catalytic performance. And the XPS result shows that 10CuZn/SBA-15 with moderate amount ZnO have the greatest ratio of $Cu^\circ/(Cu^\circ + Cu^+)$. Based on the above analysis, it can be concluded that ZnO acts as a physical barrier and the electron donor generates Cu-ZnO interaction to reduce the particle size of copper and increase the Cu° concentration, which further promotes the catalytic performance of *x*CuZn/SBA-15 in the dehydrogenation of methanol to MF.

Seen from the Table 2, the 10CuZn/SBA-15 catalyst shows a relatively higher methanol conversion of 31.1 % with the MF selectivity of 88.1 % in comparison to 10CuZn/SiO_2 (17.0 % C_{MeOH} and 59.2 % S_{MF}). This may be due to the fact that the uniformly ordered pore channels of SBA-15 facilitate the dispersion of copper, resulting in smaller particles and more exposed active sites so as to improve the catalytic performance of *x*CuZn/SBA-15. (Detailed explanations are given in the supporting information).

Fig. 9 shows the stability of 10CuZn/SBA-15 and displays the relatively stable trend of C_{MeOH} and S_{MF} with about 31 % and 89 % individually during a 100 h. The reason may be associated with prevention

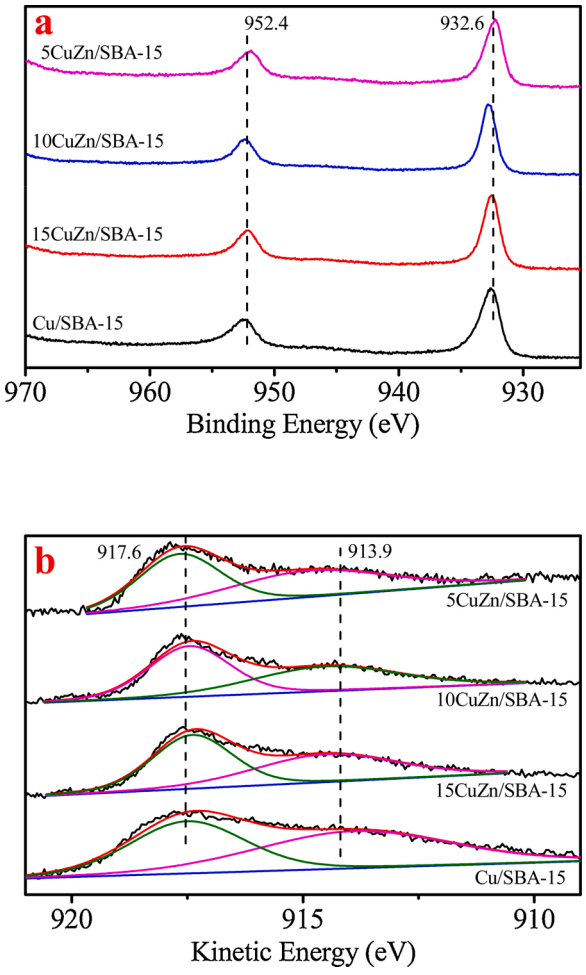

Fig. 6. (a) Cu 2p XPS and (b) Cu LMM XAES spectra of reduced catalysts.

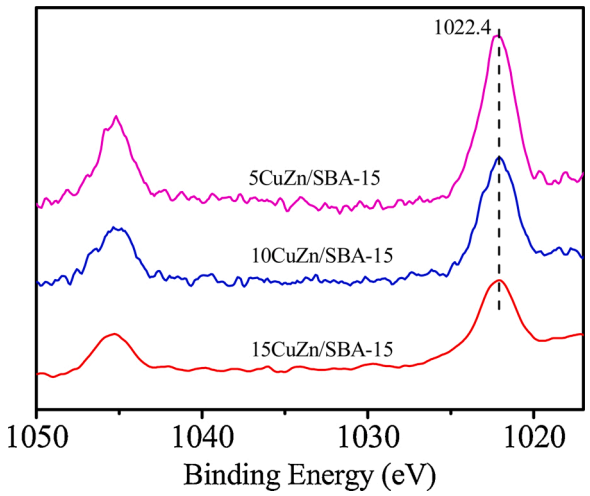

Fig. 7. Zn 2p XPS spectra of reduced catalysts.

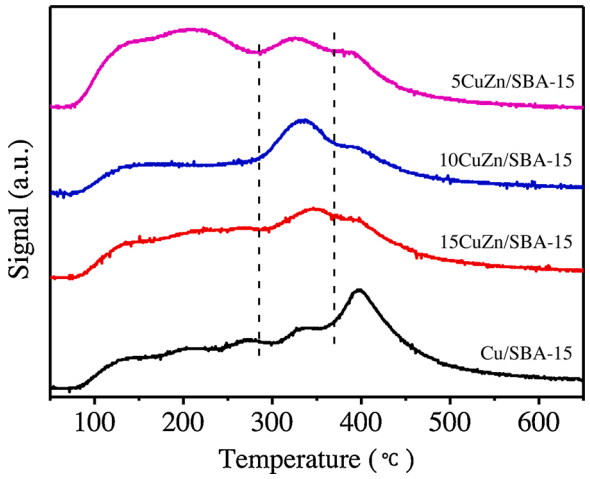

Fig. 8. CH_3OH-TPD profiles of reduced catalysts.

Table 2
The catalytic performance of reduced Cu/SBA-15 and *x*CuZn/SBA-15 catalysts.

Catalysts	C_{MeOH} (%)	S_{MF} (%)	S_{CO} (%)	S_{CO2} (%)	Y_{MF} (%)
Cu/SBA-15	17.8	46.5	52.4	1.1	8.3
15CuZn/SBA-15	23.0	55.8	42.5	1.7	12.8
10CuZn/SBA-15	31.1	88.1	10.5	1.4	27.4
5CuZn/SBA-15	24.6	70.9	27.1	2.0	17.4
10CuZn/SiO_2	17.0	59.2	39.1	1.7	10.1
Cu_5MgO_5 [54]	16.7	88.1	5.5	2.4	–
CuO-Al_2O_3 [18]	18.9	78.9	8.6	3.8	–

Reaction conditions: m_{cat}=0.3 g, T=300 °C, P_{N2} = 0.2 MPa, $LHSV_{MeOH}$=7.9 h^{-1}, 10 h.

from growth of Cu particle and the strong interaction between ZnO and Cu provided by ZnO additives, reducing the risk of catalyst deactivation and exhibiting a high thermal stability in the process of reaction.

4. Conclusions

The ordered mesoporous *x*CuZn/SBA-15 and Cu/SBA-15 catalysts are synthesized through DI method for methanol dehydrogenation to MF. It is found that appropriate amount of ZnO would take an active influence on Cu dispersion and $Cu^{\circ}/(Cu^{\circ} + Cu^{+})$ ratio in the Cu-based catalyst. Furthermore, the methanol conversion and MF selectivity increases with increasing amount of ZnO until the ratio Cu/Zn of 10, and they are highest of 31.1 % and 88.1 % respectively for 10CuZn/SBA-15,

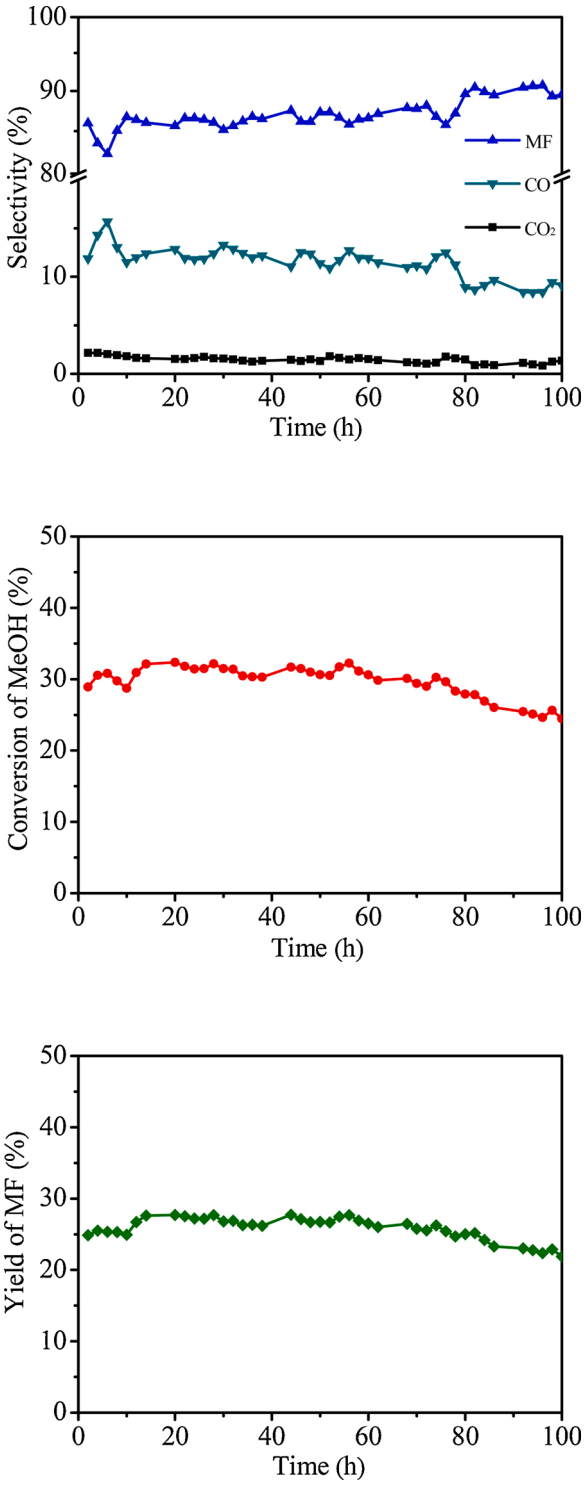

Fig. 9. Evaluation results of 10CuZn/SBA-15 stability.

which also displays satisfactory stability for longer than 100 h. The most excellent activity of 10CuZn/SBA-15 is attributed to the best dispersion of Cu particles as well as the highest $Cu^{\circ}/(Cu^{\circ} + Cu^{+})$ ratio primarily. The present work sheds light on the influence of ZnO amount in physical and chemical properties in Cu-based catalysts and highlights the importance of introduction of ZnO as a promoter to improve catalytic performance in the MF production.

CRediT authorship contribution statement

Na Wang: Conceptualization, Formal analysis, Investigation, Writing - original draft. **Yanhong Quan:** Formal analysis, Writing - review & editing. **Jinxian Zhao:** Writing - review & editing. **Haixia Li:** Conceptualization, Methodology. **Jun Ren:** Supervision, Project administration, Writing - review & editing.

Declaration of Competing Interest

The authors declare that they have no known competing financial interests or personal relationships that could have appeared to influence the work reported in this paper.

Acknowledgement

This work was funded by the National Natural Science Foundation of China (21776194 and 21808154).

Appendix A. Supplementary data

Supplementary material related to this article can be found, in the online version, at doi:https://doi.org/10.1016/j.mcat.2021.111514.

References

[1] H. Zhao, M. Lin, K. Fang, J. Zhou, Y. Sun, Preparation and evaluation of Cu-Mn/Ca-Zr catalyst for methyl formate synthesis from syngas, Appl. Catal. A Gen. 514 (2016) 276–283.
[2] A. Bakhtyari, M. Mohammadi, M.R. Rahimpour, Simultaneous production of dimethyl ether (DME), methyl formate (MF) and hydrogen from methanol in an integrated thermally coupled membrane reactor, J. Nat. Gas Sci. Eng. 26 (2015) 595–607.
[3] J.S. Lee, J.C. Kim, Y.G. Kim, Methyl formate as a new building block in C_1 chemistry, Appl. Catal. 57 (1990) 1–30.
[4] S. Jali, H.B. Friedrich, G.R. Julius, The effect of $Mo(CO)_6$ as a co-catalyst in the carbonylation of methanol to methyl formate catalyzed by potassium methoxide under CO, syngas and H_2 atmospheres. HP-IR observation of the methoxycarbonyl intermediate of $Mo(CO)_6$, J. Mol. Catal. A-Chem. 348 (2011) 63–69.
[5] Q. Zhang, C. Zhu, G. Yang, Y. Sun, D. Wang, J. Liu, High-performance microstructured Au-Ag bimetallic catalyst for oxidative coupling of methanol to methyl formate, Catal. Commun. 129 (2019), 105741.
[6] A. Vedyagin, Y. Kotolevich, P. Tsyrul'nikov, E. Khramov, A. Nizovskii, Methanol dehydrogenation over Cu/SiO_2 catalysts, Int. J. Nanotechnol. 13 (2016) 185–199.
[7] E.V. Shelepova, A.A. Vedyagin, L.Y. Ilina, A.I. Nizovskii, P.G. Tsyrulnikov, Synthesis of carbon-supported copper catalyst and its catalytic performance in methanol dehydrogenation, Appl. Surf. Sci. 409 (2017) 291–295.
[8] H. Zhao, K. Fang, J. Zhou, M. Lin, Y. Sun, Direct synthesis of methyl formate from syngas on Cu-Mn mixed oxide catalyst, Int. J. Hydrogen Energy 41 (2016) 8819–8828.
[9] J. Chen, F. Xin, S. Qin, X. Yin, Photocatalytically reducing CO_2 to methyl formate in methanol over ZnS and Ni-doped ZnS photocatalysts, Chem. Eng. J. 230 (2013) 506–512.
[10] T.P. Minyukova, I.I. Simentsova, A.V. Khasin, N.V. Shtertser, N.A. Baronskaya, A. A. Khassin, T.M. Yurieva, Dehydrogenation of methanol over copper-containing catalysts, Appl. Catal. A Gen. 237 (2002) 171–180.
[11] N. Iwasa, T. Akazawa, S. Ohyama, K. Fujikawa, N. Takezawa, Dehydrogenation of methanol to methyl formate over supported Ni, Pd and Pt catalysts. Anomalous catalytic functions of PdZn and PtZn alloys, React. Kinet. Catal. Lett. 55 (1995) 245–250.
[12] E.D. Guerreiro, O.F. Gorriz, G. Larsen, L.A. Arrúa, Cu/SiO_2 catalysts for methanol to methyl formate dehydrogenation. A comparative study using different preparation techniques, Appl. Catal. A Gen. 204 (2000) 33–48.
[13] S.P. Tenner, D.L. Trlmm, M.S. Wainwrlght, N.W. Cant, Dehydrogenation of methanol to methyl formate over copper catalysts, Ind. Eng. Chem. Prod. Res. Dev. 23 (1984) 384–388.
[14] T. Sodesawa, M. Nagacho, A. Onodera, F. Nozaki, Dehydrogenation of methanol to methyl formate over $CuSiO_2$ catatysts prepared by ion exchange method, J. Catal. 102 (1986) 460–463.
[15] F. Wang, C. Lu, Effect of coordinated ligands on catalytic properties of activated-carbon fibers-supported copper (II) complexes for the dehydrocoupling of methanol to methyl formate, Catal. Commun. 7 (2006) 709–712.
[16] E.D. Guerreiro, O.F. Gorriz, J.B. Rivarola, L.A. Arrúa, Characterization of Cu/SiO_2 catalysts prepared by ion exchange for methanol dehydrogenation, Appl. Catal. A Gen. 165 (1997) 259–271.
[17] Z. Lu, D. Gao, H. Yin, A. Wang, S. Liu, Methanol dehydrogenation to methyl formate catalyzed by SiO_2-, hydroxyapatite-, and MgO-supported copper catalysts and reaction kinetics, J. Ind. Eng. Chem. 31 (2015) 301–308.
[18] S. Sato, M. Iijima, T. Nakayama, T. Sodesawa, F. Nozaki, Vapor-phase dehydrocoupling of methanol to methyl formate over $CuAl_2O_4$, J. Catal. 169 (1997) 447–454.
[19] H. Yang, Y. Chen, X. Cui, G. Wang, Y. Cen, T. Deng, W. Yan, J. Gao, S. Zhu, U. Olsbye, J. Wang, W. Fan, A highly stable copper-based catalyst for clarifying the catalytic roles of Cu° and Cu^{+} species in methanol dehydrogenation, Angew. Chem. Int. Ed. 57 (2018) 1836–1840.
[20] D. Ji, W. Zhu, Z. Wang, G. Wang, Dehydrogenation of cyclohexanol on Cu-ZnO/SiO_2 catalysts: the role of copper species, Catal. Commun. 8 (2007) 1891–1895.
[21] Y. Zhao, B. Shan, Y. Wang, J. Zhou, S. Wang, X. Ma, An effective CuZn-SiO_2 bimetallic catalyst prepared by hydrolysis precipitation method for the hydrogenation of methyl acetate to ethanol, Ind. Eng. Chem. Res. 57 (2018) 4526–4534.
[22] X. Wang, K. Ma, L. Guo, Y. Tian, Q. Cheng, X. Bai, J. Huang, T. Ding, X. Li, Cu/ZnO/SiO_2 catalyst synthesized by reduction of ZnO-modified copper phyllosilicate for dimethyl ether steam reforming, Appl. Catal. A Gen. 540 (2017) 37–46.
[23] M. Wu, X. Hou, Y. Quan, J. Zhao, J. Ren, Catalytic hydrogenation of methyl acetate to ethanol over boron doped carbon aerogels supported Cu catalyst, ChemistrySelect 5 (2020) 11517–11521.
[24] Z. He, H. Lin, P. He, Y. Yuan, Effect of boric oxide doping on the stability and activity of a Cu-SiO_2 catalyst for vapor-phase hydrogenation of dimethyl oxalate to ethylene glycol, J. Catal. 277 (2011) 54–63.
[25] C. Liu, Y. Shang, S. Wang, X. Liu, X. Wang, J. Gui, C. Zhang, Y. Zhu, Y. Li, Boron oxide modified bifunctional Cu/Al_2O_3 catalysts for the selective hydrogenolysis of glucose to 1,2-propanediol, Mol. Catal. 485 (2020).
[26] L. Zhang, M. Meng, S. Zhou, Z. Sun, J. Zhang, Y. Xie, T. Hu, Promotional effect of partial substitution of Zn by Ce in CuZnAlO catalysts used for hydrogen production via steam reforming of dimethyl ether, J. Power Sources 232 (2013) 286–296.
[27] M. Huang, G. Li, G. Li, Catalytic activity of dehydrogenation of methanol to MF over Cu/SBA-15 and Cu-ZnO/SBA-15 prepared by grinding and impregnation, Adv. Mater. Res. 608–609 (2013) 1476–1479.
[28] L. Chen, P. Guo, L. Zhu, M. Qiao, W. Shen, H. Xu, K. Fan, Preparation of Cu/SBA-15 catalysts by different methods for the hydrogenolysis of dimethyl maleate to 1,4-butanediol, Appl. Catal. A Gen. 356 (2009) 129–136.
[29] V. Boosa, V. Bilakanti, V.K. Velisoju, N. Gutta, S. Inkollu, V. Akula, An insight on the influence of surface Lewis acid sites for regioselective C-H bond C_3-cyanation of indole using NH_4I and DMF as combined cyanide source over Cu/SBA-15 catalyst, Mol. Catal. 445 (2018) 43–51.
[30] Z. Xia, H. Liu, H. Lu, Z. Zhang, Y. Chen, High selectivity of cyclohexane dehydrogenation for H_2 evolution over Cu/SBA-15 catalyst, Catal. Lett. 147 (2017) 1295–1302.
[31] W. Tian, L. Sun, X. Song, X. Liu, Y. Yin, G. He, Adsorptive desulfurization by copper species within confined space, Langmuir 26 (2010) 17398–17404.
[32] H. Yang, P. Gao, C. Zhang, L. Zhong, X. Li, S. Wang, H. Wang, W. Wei, Y. Sun, Core-shell structured Cu@m-SiO_2 and Cu/ZnO@m-SiO_2 catalysts for methanol synthesis from CO_2 hydrogenation, Catal. Commun. 84 (2016) 56–60.
[33] Y. Zhao, Z. Guo, H. Zhang, Y. Xu, Y. Wang, J. Zhang, Y. Xu, S. Wang, X. Ma, Ordered mesoporous CuZn/HPS catalysts for the chemoselective hydrogenation of dimethyl adipate to 1,6-hexan-ediol, Chem. Lett. 46 (2017) 1079–1082.
[34] T. Lunkenbein, J. Schumann, M. Behrens, R. Schlögl, M.G. Willinger, Formation of a ZnO overlayer in industrial $Cu/ZnO/Al_2O_3$ catalysts induced by strong metal-support interactions, Angew. Chem. Int. Ed. 54 (2015) 4544–4548.
[35] G. Laugel, J. Arichi, H. Guerba, M. Molière, A. Kiennemann, F. Garin, B. Louis, Co_3O_4 and Mn_3O_4 nanoparticles dispersed on SBA-15: efficient catalysts for methane combustion, Catal. Lett. 125 (2008) 14–21.
[36] S. Zander, E.L. Kunkes, M.E. Schuster, J. Schumann, G. Weinberg, D. Teschner, N. Jacobsen, R. Schlögl, M. Behrens, The role of the oxide component in the development of copper composite catalysts for methanol synthesis, Angew. Chem. Int. Ed. 52 (2013) 6536–6540.
[37] I. Kasatkin, P. Kurr, B. Kniep, A. Trunschke, R. Schlögl, Role of lattice strain and defects in copper particles on the activity of $Cu/ZnO/Al_2O_3$ catalysts for methanol synthesis, Angew. Chem. Int. Ed. 119 (2007) 7465–7468.
[38] T. Fujitani, J. Nakamura, The effect of ZnO in methanol synthesis catalysts on Cu dispersion and the specific activity, Catal. Lett. 56 (1998) 119–124.
[39] M. Behrens, Meso- and nano-structuring of industrial $Cu/ZnO/(Al_2O_3)$ catalysts, J. Catal. 267 (2009) 24–29.
[40] A.J. Marchi, J.L.G. Fierro, J. Santamaría, A. Monzón, Dehydrogenation of isopropylic alcohol on a Cu/SiO_2 catalyst: a study of the activity evolution and reactivation of the catalyst, Appl. Catal. A Gen. 142 (1996) 375–386.
[41] L. Chen, P. Guo, M. Qiao, S. Yan, H. Li, W. Shen, H. Xu, K. Fan, Cu/SiO_2 catalysts prepared by the ammonia-evaporation method: texture, structure, and catalytic performance in hydrogenation of dimethyl oxalate to ethylene glycol, J. Catal. 257 (2008) 172–180.
[42] D. Wang, J. Zhao, H. Song, L. Chou, Characterization and performance of $Cu/ZnO/Al_2O_3$ catalysts prepared via decomposition of M(Cu,Zn)-ammonia complexes under sub-atmospheric pressure for methanol synthesis from H_2 and CO_2, J. Nat. Gas Chem. 20 (2011) 629–634.
[43] A. García-Trenco, A. Vidal-Moya, A. Martínez, Study of the interaction between components in hybrid CuZnAl/HZSM-5 catalysts and its impact in the syngas-to-DME reaction, Catal. Today 179 (2012) 43–51.
[44] Y. Wang, W. Yang, D. Yao, S. Wang, Y. Xu, Y. Zhao, X. Ma, Effect of surface hydroxyl group of ultra-small silica on the chemical states of copper catalyst for dimethyl oxalate hydrogenation, Catal. Today 350 (2020) 127–135.
[45] H. Huang, B. Wang, Y. Wang, Y. Zhao, S. Wang, X. Ma, Partial hydrogenation of dimethyl oxalate on Cu/SiO_2 catalyst modified by sodium silicate, Catal. Today 358 (2020) 68–73.

[46] X. Li, Y. Wang, X. Wei, Y. Zhao, Effect of Na promoter on the catalytic performance of Pd-Cu/hydroxyapatite catalyst for room-temperature CO oxidation, Mol. Catal. 491 (2020).
[47] D. Yao, Y. Wang, Y. Li, Y. Zhao, J. Lv, X. Ma, A high-performance nanoreactor for carbon-oxygen bond hydrogenation reactions achieved by the morphology of nanotube-assembled hollow spheres, ACS Catal. 8 (2018) 1218–1226.
[48] Y. Zhao, S. Li, Y. Wang, B. Shan, J. Zhang, S. Wang, X. Ma, Efficient tuning of surface copper species of Cu/SiO_2 catalyst for hydrogenation of dimethyl oxalate to ethylene glycol, Chem. Eng. J. 313 (2017) 759–768.
[49] W. Di, J. Cheng, S. Tian, J. Li, J. Chen, Q. Sun, Synthesis and characterization of supported copper phyllosilicate catalysts for acetic ester hydrogenation to ethanol, Appl. Catal. A Gen. 510 (2016) 244–259.
[50] G.U. Kulkarni, C.N.R. Rao, EXAFS and XPS investigations of Cu/ZnO catalysts and their interaction with CO and methanol, Top. Catal. 22 (2003) 183–189.
[51] Y. Matsumura, H. Ishibe, Suppression of CO by-production in steam reforming of methanol by addition of zinc oxide to silica-supported copper catalyst, J. Catal. 268 (2009) 282–289.
[52] R. Zhang, Y. Sun, S. Peng, In situ FTIR studies of methanol adsorption and dehydrogenation over Cu/SiO_2 catalyst, Fuel 81 (2002) 1619–1624.
[53] N.W. Cant, S.P. Tonner, D.L. Trimm, M.S. Wainwright, Isotopic labeling studies of the mechanism of dehydrogenation of methanol to methyl formate over copper-based catalysts, J. Catal. 91 (1985) 197–207.